Consistent anharmonic-shell-model calculation for the Raman mode in silicon

S. Koval and R. Migoni
Departamento de Física, Facultad de Ciencias Exactas, Ingeniería y Agrimensura (Universidad de Rosario) and Instituto de Física Rosario (Consejo Nacional de Investigaciones Científicas y Técnicas, Universidad de Rosario), Bv. 27 de Febrero 210 Bis, 2000 Rosario, Argentina
(Received 12 January 1993; revised manuscript received 3 June 1993)

We show that a previous failure to describe the frequency shift Δ and linewidth Γ of the optical zone-center mode in silicon with an anharmonic shell model arises from the neglect of the electronic polarizability effects in the perturbative treatment of the anharmonic interactions. We consider cubic anharmonic shell-shell interactions between nearest-neighbor atoms in a shell model used in the past for silicon. We apply an anharmonic perturbation theory which properly takes into account the adiabatic constraint for the shell's polarization. We obtain Δ and Γ as functions of temperature in good agreement with experimental data.

I. INTRODUCTION

The simulation of electronic polarizability effects in lattice dynamics is most commonly made with the shell model (SM).[1-3] Here, the adiabatic condition for the electrons is represented by equilibrium conditions of massless shells for every instantaneous core configuration. Such constraints give rise to effective long-range core-core interactions and must be considered in the perturbative development of the phonon self-energy due to anharmonic interactions between shells of neighboring ions.[4] Thus, important corrections over a perturbation theory for anharmonic interactions between effectively rigid ions are obtained. By taking a monoatomic chain as a test, we have recently shown that those corrections are significant for the wave-vector dependence of the phonon frequency shift and linewidth as well as for the ratio between these quantities.[5]

An anharmonic SM has been applied quite a long time ago for the calculation of anharmonic effects on the long-wave optical phonon (the Raman mode) in silicon.[6] Although the bare phonons were obtained from the SM,[7,8] the anharmonic effects are calculated through the usual perturbative formalism,[9] which considers anharmonic force constants between point ions. With cubic force constants fitted to thermal expansion data, a frequency shift in good agreement with experience was obtained, but the linewidth comes up an order of magnitude larger than the observed value. This discrepancy was more recently discussed, although not clarified, by Haro *et al.*[10] They obtain satisfactory results from a model which includes harmonic long-range nonlocal dipole interactions, while the anharmonic interactions are incorporated as in the previous work.[6] Other calculations of the Raman mode self-energy in Si do not take into account electronic polarizability effects explicitly either in the harmonic nor in the anharmonic part.[11,12] The various results have been recently reviewed.[13]

Our one-dimensional calculation[5] allowed us to anticipate that the above-mentioned failure of the anharmonic SM for Si may be ascribed to the neglect of the long-range polarizability effects in the perturbative treatment of the anharmonic interactions. We address this question in this paper by applying the developed perturbative formalism to the calculation of the linewidth and lineshift of the Raman mode in Si with the realistic anharmonic SM.

The electronic polarizability effects on the lattice dynamics of the homopolar covalent materials are better described by the bond-charge model.[14] However, a calculation of the anharmonic phonon self-energy has not been attempted with this model.

II. THE MODEL

We started from the harmonic SM of Refs. 7 and 8 (best fit) to calculate the eigenvectors and frequencies of the phonon modes. Since the parameter α_T of the model is not specified in Ref. 7 or 8 we take $\alpha_T=\alpha_S$. Also we modified slightly the parameter π_1 in order to improve the fit. The model reproduces satisfactorily the experimental data for the principal symmetry directions.

In the next step, we attempted to obtain the anharmonic parameters used by Cowley and co-workers[6,8] for the cubic interaction but we didn't succeed. First, one can show that the parameter B of Dolling and Cowley[8] vanishes identically for a nearest-neighbor central interaction, in contradiction to their result that B is different from zero. This was also pointed out in Ref. 10. Second, it is not possible to derive an expression for the Grüneisen constant $\gamma(\mathbf{q}j)$ in terms of the parameters A and B defined in Ref. 8. For these reasons, we were not able to compare our results directly with Cowley's calculation. Therefore, we determined the cubic central force constants $\phi_{\alpha\beta\gamma}(0\kappa,l\kappa')$ from experimental data and performed the calculation with the anharmonic SM and also with the expressions for the usual perturbation theory.[9] $(l\kappa\alpha)$ denote the unit cell, atomic site, and Cartesian index, respectively. The parameters $C=\phi'''/R^3-3D/R^2$ and $D=\phi''/R^2-\phi'/R^3$, which determine $\phi_{\alpha\beta\gamma}(0\kappa,l\kappa')$,[15] are evaluated using the expression of the optic mode Grüneisen constant $\gamma(\mathbf{0}j)$,[16] with ϕ''' obtained from the second- and third-order elastic constants.[10] From the ex-

perimental values of $\gamma(0j)$ (Ref. 17) and the elastic constants (Ref. 18) we obtain $C=14.27e^2/v\text{Å}^4$ and $D=-42.08e^2/v\text{Å}^2$, where v is the primitive cell volume.

The anharmonic SM is essentially the same as the one defined in Ref. 5 but it is developed in three dimensions and we also add up the Coulomb interaction to the harmonic part of the potential. The whole crystal potential is written in the following way:

$$\begin{aligned}\phi(\mathbf{u},\mathbf{v})=&\sum_{ij}\{\tfrac{1}{2}\phi_{ij}^{D}u_iu_j+\phi_{ij}^{F}u_iv_j+\tfrac{1}{2}\phi_{ij}^{S}v_iv_j\}\\&+\sum_{ij}{}'\tfrac{1}{2}\phi_{ij}^{C}Y^2\{v_iv_j-2v_iv_j+u_iu_j\}\\&+\phi_3(\mathbf{v})+\phi_4(\mathbf{v}),\end{aligned}\tag{2.1}$$

where $\phi_3(\mathbf{v})$, $\phi_4(\mathbf{v})$ are, respectively, the cubic and quartic shell-shell interaction for a nearest-neighbor two-body central potential. We denote $i\equiv(l\kappa\alpha)$. ϕ^D, ϕ^F, and ϕ^S are the short-range core-core, core-shell, and shell-shell interactions, respectively. u_i,v_i denote the core and absolute shell displacements. ϕ^C is the Coulomb force constant and Y is the shell charge of the ion. We recall that the total ionic charge is equal to zero. The prime in the second term of (2.1) means that the summation runs over $(l'\kappa')\neq(l\kappa)$. The general form of the matrices ϕ^D, ϕ^F, and ϕ^S for first and second neighbors are given in the Appendix. The values of the parameters are reproduced in Table I. The polarizability parameters are $Y=-4.6e$ for the shell charge and $K=356.1$ (e^2/v) for the core-shell coupling constant of the ion.

Following the procedure of Ref. 5 for developing the perturbation theory up to second order with the potential of Eq. (2.1), we find that the diagrammatic expansion for the phonon self-energy is

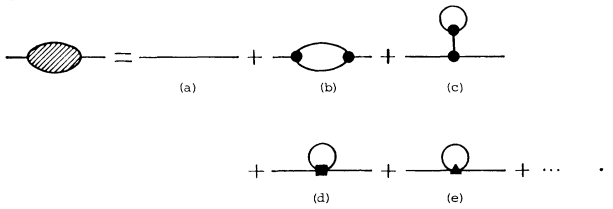

(2.2)

After replacing the expressions for each diagram, we obtain (with the same ordering)

$$\begin{aligned}=&g_{ij}+\tfrac{1}{2}g_{iq}X^{(3)}_{(qlp)}g_{lt}g_{ph}X^{(3)}_{(ths)}g_{sj}\\&+\tfrac{1}{2}g_{iq}X^{(3)}_{(qlp)}g_{pt}g_{hs}X^{(3)}_{(ths)}g_{lj}\\&-\tfrac{1}{2}g_{iq}X^{(4)}_{(qklm)}g_{kl}g_{mj}\\&+\tfrac{3}{2}g_{iq}Z_{(qklm)}g_{kl}g_{mj},\end{aligned}\tag{2.3}$$

where g_{ij} is the free phonon propagator in direct space (a parenthesis means symmetrization in the enclosed indices). The vertices denoted by a dot, square, and triangle correspond to $X^{(3)}$, $X^{(4)}$, and Z, respectively, whose expressions are given in the Appendix. As it can be seen there, the effective quartic vertex of diagram (e) arises actually from cubic anharmonic shell-shell interactions and is peculiar to the SM.

Diagram (c) in the series (2.2) has a vanishing contribution for a crystal with every atom at an inversion center. Even though the silicon crystal does not possess this symmetry, it can be seen that the coefficient $X^{(3)}(0j,0j_1,0j_2)$ corresponding to the vertices of (c) vanishes unless j,j_1,j_2 refer to three different optical branches. Therefore, diagram (c) does not contribute for silicon, as it was previously pointed out.[10]

It follows that the frequency shift Δ and linewidth Γ for the zone-center optical mode in silicon are given by

$$\Delta(0j,\omega)=\Delta^{(b)}(0j,\omega)+\Delta^{(d)}(0j)+\Delta^{(e)}(0j)+\Delta^{TE}(0j)\tag{2.4}$$

and

$$\Gamma(0j,\omega)=\Gamma^{(b)}(0j,\omega),\tag{2.5}$$

where

$$\Delta^{(b)}(0j,\omega)=-\frac{\hbar}{16N}\sum_{\mathbf{q}j_1j_2}|X^{(3)}(0j,\mathbf{q}j_1,-\mathbf{q}j_2)|^2\times\mathcal{P}(\omega,\omega^0(\mathbf{q}j_1),\omega^0(\mathbf{q}j_2)),\tag{2.6}$$

$$\Delta^{(e)}(0j)=-\frac{\hbar}{8N}\sum_{\mathbf{q}j_1}(2n(\mathbf{q}j_1)+1)\times\{2Z(0j,\mathbf{q}j_1,-\mathbf{q}j_1,0j)+Z(0j,0j,\mathbf{q}j_1,-\mathbf{q}j_1)\},\tag{2.7}$$

$$\Delta^{(d)}(0j)=\frac{\hbar}{8N}\sum_{\mathbf{q}j_1}[2n(\mathbf{q}j_1)+1]X^{(4)}(0j,0j,\mathbf{q}j_1,-\mathbf{q}j_2),\tag{2.8}$$

$$\Delta^{\text{TE}}(0j)=\omega(0j)\left\{\exp\left[-3\gamma(0j)\int_0^T\alpha(T')dT'\right]-1\right\},\tag{2.9}$$

and

$$\Gamma^{(b)}(0j,\omega)=\frac{\pi\hbar}{16N}\sum_{\mathbf{q}j_1j_2}|X^{(3)}(0j,\mathbf{q}j_1,-\mathbf{q}j_2)|^2\times\mathcal{D}(\omega,\omega^0(\mathbf{q}j_1),\omega^0(\mathbf{q}j_2)).\tag{2.10}$$

N is the number of q points sampled in the Brillouin zone and $n(\mathbf{q}j)$ is the Bose occupation number. Equation (2.4) includes the thermal-expansion contribution Δ^{TE} to the lineshift, where $\alpha(T)$ in Eq. (2.9) is the thermal-expansion

TABLE I. Harmonic force-constant parameters for the first (α and β) and second neighbors in silicon. Unit: e^2/v.

	α	β	μ	ν	δ	λ
ϕ^D	−7.797	−4.473	0.264	−0.298	−0.619	0.800
ϕ^F	0.000	9.320	0.000	0.000	0.000	0.000
ϕ^S	29.217	−9.583	−0.989	1.116	2.319	−2.999

coefficient.[11] The functions $\mathcal{P}$ and $\mathcal{D}$ are defined in the Appendix.

All previous perturbative calculations of phonon frequency shifts and linewidths consider anharmonic force constants which arise from a Born-von Karman development of the crystal potential in powers of the nuclear displacements. Thus the ions are taken as effectively rigid units and therefore we shall call this the rigid-ion (RI) perturbative approach. This treatment has been applied[6] even in cases where the bare phonon frequencies were obtained from a harmonic model which explicitly takes into account electronic polarizability effects. Such approach corresponds to perform the limit $K \to \infty$ in the expressions for the vertices given in the Appendix except in the eigenvectors and frequencies. This leads to $S^{-1}_{\alpha\beta}(\kappa\kappa',\mathbf{q}) \to 0$ and $C_{\alpha\beta}(\kappa\kappa',\mathbf{q}) \to -\delta_{\alpha\beta}\delta_{\kappa\kappa'}$. In this way we recover the expressions of the usual perturbation theory[9] and the term $\Delta^{(e)}$ vanishes. Note that the expressions (A3) and (A4) for the vertices in diagrams (b), (c), and (d) are analogous to the ones of Ref. 9, except that the core eigenvectors $\mathbf{e}(\mathbf{q}j)$ are replaced by the shell ones $C(\mathbf{q})\mathbf{e}(\mathbf{q}j)$.

III. RESULTS AND DISCUSSIONS

Cowley has pointed out[6] that the quartic anharmonic contribution $\Delta^{(d)}$ nearly cancels the thermal-expansion contribution Δ^{TE} within the RI perturbative approach. On the other hand, we expect that the result for the SM expression of $\Delta^{(d)}$ [Eq. (2.8)] is much smaller than the result obtained from the RI theory.[5] Therefore, since Δ^{TE} is already a minor contribution, we neglect the quartic term $\Delta^{(d)}$ in Eq. (2.4) for the lineshift but retain Δ^{TE}.

For the numerical evaluation of the frequency shift $\Delta(\mathbf{0}j,\omega)$, and the linewidth $\Gamma(\mathbf{0}j,\omega)$, we sampled 111 points in the irreducible one-forty-eighth portion of the Brillouin zone. We also took into account the Umklapp processes. We have chosen the following representation of the δ function:

$$\delta(\omega) = \lim_{\epsilon \to 0} \left\{ \frac{\epsilon}{\pi(\omega^2+\epsilon^2)} \right\}, \tag{3.1}$$

and for the principal part,

$$\left\{ \frac{1}{\omega} \right\}_P = \lim_{\epsilon \to 0} \left\{ \frac{\omega}{\omega^2+\epsilon^2} \right\} \tag{3.2}$$

with small but finite values of ϵ. The calculated values of Δ and Γ are independent of ϵ within certain intervals. We select $\epsilon_\Gamma = 6\ \mathrm{cm}^{-1}$ and $\epsilon_\Delta = 2\ \mathrm{cm}^{-1}$ for the δ function and principal part representation, respectively, values which lie in the center of such intervals.

The third-order force constants $\phi_{\alpha\beta\gamma}(0\kappa,l'\kappa')$ were evaluated with the anharmonic parameters C and D derived from experimental data as explained at the beginning of Sec. II.

In Table II we show the different contributions to the frequency shift $\Delta(\mathbf{0}j,\omega)$ for the zone-center optical mode $\omega = \omega(\mathbf{0}j)$ at 300 K. We have used the experimental data of Ref. 19 for the thermal-expansion coefficient as a function of temperature $\alpha(T)$ to evaluate Δ^{TE} for silicon. We also display the limit to the RI perturbation theory $\Delta^{(b)}_{\mathrm{RI}}$ for the (b) diagram. We see in Table II that the values of the total linewidth for our SM anharmonic treatment are substantially smaller than those for the RI limit. This was also found with the simple one-dimensional model.[5] We also observe that the new contribution to the lineshift $\Delta^{(e)}$ obtained when the shell polarization effects are properly taken into account in the perturbative development of the phonon propagator, is comparable in magnitude to the contribution $\Delta^{(b)}_{\mathrm{SM}}$ of the same theory.

TABLE II. The various contributions to the frequency shift (cm^{-1}) at 300 K for the SM perturbation theory and the RI limit. Δ is the total frequency shift.

	$\Delta^{(b)}$	$\Delta^{(e)}$	Δ^{TE}	Δ
SM	−2.631	−1.646	−0.288	−4.565
RI	−30.497	0.000	−0.288	−30.785

In Fig. 1, we plot the frequency shift difference $\Delta(T)-\Delta(0)$ as a function of temperature. We can see that the agreement of the anharmonic SM theory (solid triangles) with the experimental data[20] (open circles) is quite good below 500 K. If the thermal-expansion term is not included the agreement is less satisfactory (solid squares). The increasing discrepancy between experiment and theory, particularly noticeable above 500 K, is due to the neglect of fourth-order anharmonic terms arising from quartic anharmonic interactions in second-order or cubic anharmonicities in fourth order of perturbation theory. These terms correspond to diagrams with vertex corrections,

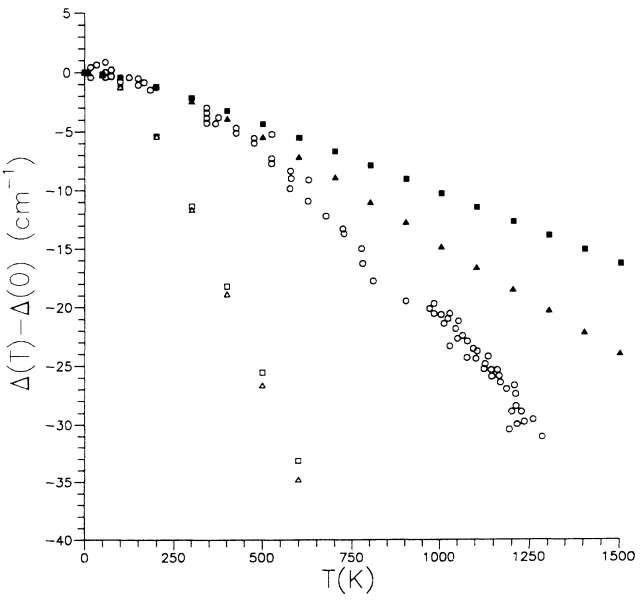

FIG. 1. Frequency shift difference of the Raman model in silicon versus temperature: experimental data (○), SM perturbation theory for cubic anharmonicity including thermal expansion (▲) and without it (■), RI limit of the perturbation theory with thermal expansion (△) and without it (□).

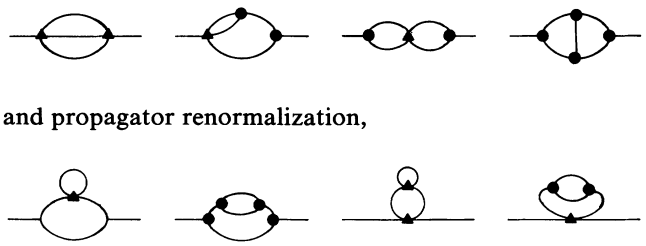

and propagator renormalization,

We recall that the effective quartic vertex ▲ arises from cubic shell-shell interactions. Additional diagrams, with vertices ■ instead of ▲ above, would contribute to the same order if quartic anharmonicity were included. The experimental data[20] in Fig. 1 show a nonlinear dependence with T up to the highest temperatures. The terms we have calculated, as well as the neglected quartic anharmonicity in first order [diagram (d) in Eq. (2.2)], are all linear in the phonon occupation numbers and thus lead to a linear temperature dependence of the self-energy at high temperatures. The just mentioned neglected terms of higher order, on the other hand, are quadratic in the occupation number and thus would provide the necessary corrections at high temperatures. This has been clearly shown by empirical fits in Ref. 13. Our results are similar to those of Ref. 10, which were obtained with a RI scheme for the harmonic model with the inclusion of short-range forces up to fourth neighbors and long-range nonlocal dipole interactions. These long-range interactions are generated implicity in a SM and have a direct physical interpretation. In order to compare with Cowley's results,[6] we performed the RI limit in the expressions of $\Delta(0j,\omega)$ without including the thermal-expansion contribution Δ^{TE}. We obtain the values represented by open squares in Fig. 1 which, in contrast with Cowley's calculations, differ significantly with the experiment. This discrepancy must be ascribed to the previously mentioned inconsistencies of Cowley's expressions which lead us to a determination of the anharmonic parameters. We also show through open triangles that the inclusion of the thermal-expansion contributions leads to even worse results in this limit.

We have also calculated the phonon linewidth with the help of Eq. (2.10). The results for 2Γ are shown in Fig. 2 as a function of temperature. We observe that the consistent anharmonic SM theory leads to results (solid squares) in good agreement with the experiment[20] up to temperatures of the order of 750 K. Above this temperature, the nonlinear behavior of the experimental data is more pronounced and the failure of the theory is related to the neglect of fourth-order anharmonic process. We also performed the RI limit in 2Γ (open squares) and obtained a discrepancy similar to that of Cowley: The results lie an order of magnitude above the experimental data.

In Fig. 3 we plot the frequency dependence of the $\Delta^{(b)}$ contribution to the lineshift at 10 K. The term $\Delta^{(e)}$ peculiar to the SM is frequency independent. The results for the RI limit are considerably larger than those of the anharmonic SM in the whole frequency range. The typical dispersive behavior is essentially the same for both cases, which reflects the fact that only the vertices are

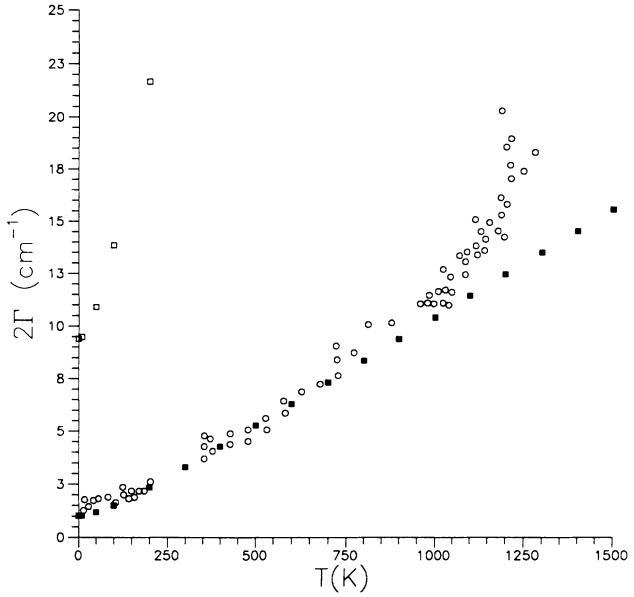

FIG. 2. Linewidth of the Raman mode in silicon versus temperature: experimental data (○), SM perturbation theory for cubic anharmonicity (■) and RI limit of the theory (□).

modified when taking the RI limit. The frequency shift is negative up to frequencies of the order of 650 cm^{-1} for both models. At higher frequencies, the SM results are positive, while the RI limit shows negative values of $\Delta^{(b)}$ between 850 and 1000 cm^{-1}. At higher temperatures, we observe in both cases that the magnitude of $\Delta^{(b)}$ increases specially for low frequencies but the qualitative behavior remains unchanged.

We calculated the linewidth as a function of frequency at several temperatures. In Fig. 4, we show the results at

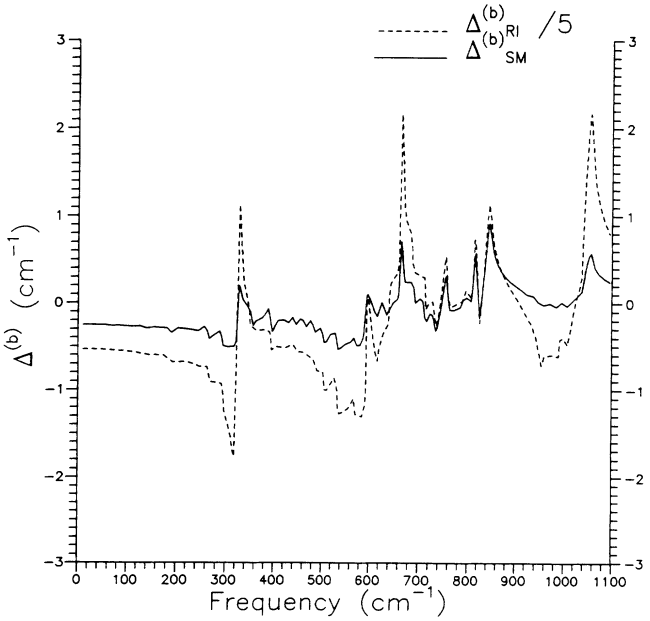

FIG. 3. Frequency dependence of contribution (b) to the frequency shift in silicon at 10 K: SM perturbation theory (——) and RI limit of the theory (— — —).

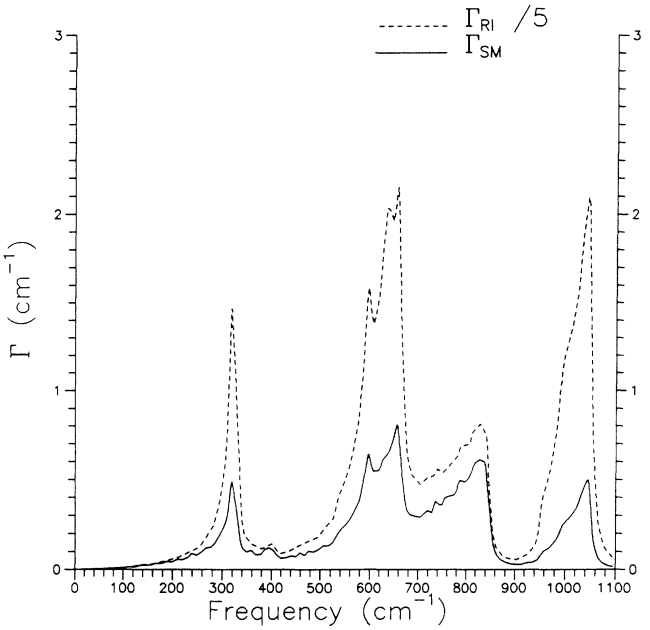

FIG. 4. Frequency dependence of the damping constant Γ in silicon at 10 K: SM perturbation theory for cubic anharmonicity (——) and RI limit of the theory (— — —).

10 K. We observe that the dispersive behavior is the same for both models, but the RI limit exhibits much larger magnitudes than the SM results in all the frequency ranges considered. We observe three bands according to various two-phonon combinations. The lower band centered around ~ 320 cm^{-1} corresponds to 2 TA. The second band around ~ 620 cm^{-1} is due to LO-TA and TO-TA combinations and exhibits the highest peak at 650 cm^{-1} for both models. Finally, the upper band around 1040 cm^{-1} corresponds to transitions to LO-TO phonon combinations. Each peak in Γ is clearly related to a resonantlike feature in Fig. 3. With increasing temperature we find the same behavior as in the case of $\Delta^{(b)}$.

The overall smaller intensities of the SM compared with the RI limit in both Fig. 3 and 4 are due to the fact that the variation of the intershell distances caused by core displacements is attenuated by the core-shell polarization. Therefore, the effects of anharmonic interactions between shells is weaker the softer the core-shell interaction. It can be seen that the absolute shell displacements, which enter through (A7) in the expressions of the vertices, are in general smaller than the core displacement amplitudes. On the other hand, the attenuation of the shell displacements depends on the form of the core eigenvector and therefore becomes indirectly frequency dependent. This effect leads to intensity ratios for distinct frequencies in the SM different from the corresponding ratios in the RI limit, as can be seen in Fig. 3 and 4.

IV. CONCLUSIONS

We have shown that a proper treatment of the electronic polarizability effects, while performing the anharmonic perturbation theory for the shell model, leads to a good description of the phonon frequency shift and linewidth in silicon. The results are substantially different from the ones obtained with the usual anharmonic perturbation theory, where the anharmonicity is taken between effectively rigid ions. In particular this explains the big discrepancy with experimental data obtained previously for the linewidth of the zone-center optical phonon in silicon with a shell model.[6] Our results still show discrepancies at high temperatures which are due to the neglect of fourth-order anharmonic terms, which lead to a T^2 dependence of $\Delta(T)$ and $\Gamma(T)$. Compared with the results which Haro *et al.*[10] obtained with a more complicated harmonic model, our results are of similar quality for the frequency shift and slightly better for the linewidth.

Finally, we wish to point out that an analogous treatment of anharmonic interactions in the calculation of phonon self-energies should be developed for other models which explicitly include degrees of freedom for the description of electronic polarizability effects, like the bond-charge model. An anharmonic version of this model has been applied to the study of the mode Grüneisen constants in Si.[21] These, however, retain their usual expressions due to the fact that the phonon frequency changes upon strain do not contain contributions from polarizations of bond charges, which remain at the inversion centers in the Si structure when this is homogeneously deformed. Also our application of the usual expression of the Grüneisen constant for the determination of the anharmonic parameters in the shell model is allowed by the fact that no contribution of shell polarizations will arise in Si. In fact an isotropic volume change does not distort the coordination tetrahedra around each atom, and therefore does not induce any shell displacement.

ACKNOWLEDGMENTS

We especially thank A. Greco for stimulating ideas and acknowledge helpful discussions with M. Stachiotti and A. Dobry. We also acknowledge support from Consejo Nacional de Investigaciones Científicas y Técnicas.

APPENDIX

The general form of the matrices ϕ^D, ϕ^F, and ϕ^S for first and second neighbors are, respectively, first neighbors:

$$\phi(111)=\begin{bmatrix}\alpha & \beta & \beta\\ \beta & \alpha & \beta\\ \beta & \beta & \alpha\end{bmatrix}, \tag{A1}$$

second neighbors:

$$\phi(110)=\begin{bmatrix}\mu & \nu & -\delta\\ \nu & \mu & -\delta\\ \delta & \delta & \lambda\end{bmatrix}, \tag{A2}$$

where (111) means the atom located at the coordinate $(1,1,1)a/4$ and (110) correspond to $(1,0,0)a/2$, a is the lattice constant.

The expressions for the vertices in the reciprocal space are

$$X^{(3)}(\mathbf{q}_1 j_1,\mathbf{q}_2 j_2,\mathbf{q}_3 j_3)=\frac{1}{2\times 3!}\sum_{l\kappa}\sum_{l'\kappa'}\sum_{\alpha_1\alpha_2\alpha_3}\phi_{\alpha_1\alpha_2\alpha_3}(l\kappa,l'\kappa')\prod_{n=1}^{3}\mathcal{J}_n(l\kappa,l'\kappa')\ , \tag{A3}$$

$$X^{(4)}(\mathbf{q}_1 j_1,\mathbf{q}_2,j_2,\mathbf{q}_3 j_3,\mathbf{q}_4 j_4)=\frac{1}{2\times 4!}\sum_{l\kappa}\sum_{l'\kappa'}\sum_{\alpha_1\alpha_2\alpha_3\alpha_4}\phi_{\alpha_1\alpha_2\alpha_3\alpha_4}(l\kappa,l'\kappa')\prod_{n=1}^{4}\mathcal{J}_n(l\kappa,l'\kappa')\ , \tag{A4}$$

$$\begin{aligned}Z(\mathbf{q}_1 j_1,\mathbf{q}_2 j_2,\mathbf{q}_3 j_3,\mathbf{q}_4 j_4)=&\frac{1}{2\times 3!\times 3!}\sum_{l_1\kappa_1}\sum_{l_2\kappa_2}\sum_{l_3\kappa_3}\sum_{l_4\kappa_4}\sum_{\alpha\alpha_1\alpha_2}\sum_{\beta\alpha_3\alpha_4}\phi_{\alpha\alpha_1\alpha_2}(l_1\kappa_1,l_2\kappa_2)\\&\times\phi_{\beta\alpha_3\alpha_4}(l_3\kappa_3,l_4\kappa_4)\left[\sum_{r=1}^{2}\sum_{s=3}^{4}S^{-1}_{\alpha\beta}(\kappa_r\kappa_s,-\mathbf{q}_1-\mathbf{q}_2)(-1)^{r+s}\exp[(-\mathbf{q}_1-\mathbf{q}_2)r(l_r\kappa_r,l_s\kappa_s)]\right]\\&\times\left\{\prod_{n=1}^{2}\mathcal{J}_n(l_1\kappa_1,l_2\kappa_2)\right\}\left\{\prod_{m=3}^{4}\mathcal{J}_m(l_3\kappa_3,l_4\kappa_4)\right\}\ ,\end{aligned} \tag{A5}$$

where we have made the following definitions:

$$\mathcal{J}_n(l\kappa,l'\kappa')\equiv E_{\alpha_n}(\kappa,\mathbf{q}_n j_n)\exp\{i\mathbf{q}_n\mathbf{r}(l\kappa)\}-E_{\alpha_n}(\kappa',\mathbf{q}_n j_n)\exp\{i\mathbf{q}_n\mathbf{r}(l'\kappa')\}\ , \tag{A6}$$

$$E_{\alpha_n}(\kappa,\mathbf{q}_n j_n)\equiv\sum_{\beta\kappa'}\frac{C_{\alpha_n\beta}(\kappa\kappa',\mathbf{q}_n)e_\beta(\kappa',\mathbf{q}_n j_n)}{\sqrt{M_\kappa\omega^0(\mathbf{q}_n j_n)}}\ , \tag{A7}$$

and the matrix C is

$$C_{\alpha\beta}(\kappa\kappa',\mathbf{q})=\sum_{\gamma\kappa''}S^{-1}_{\alpha\gamma}(\kappa\kappa'',\mathbf{q})F_{\beta\gamma}(\kappa'\kappa'',\mathbf{q})\ , \tag{A8}$$

where

$$S^{-1}_{\alpha\gamma}(\kappa\kappa'',\mathbf{q})=\{\phi^S_{\alpha\beta}(\kappa\kappa',\mathbf{q})+Y^2\phi^C_{\alpha\beta}(\kappa\kappa',\mathbf{q})+K\delta_{\alpha\beta}\delta_{\kappa\kappa'}\}^{-1} \tag{A9}$$

and

$$F_{\alpha\beta}(\kappa\kappa'',\mathbf{q})=\phi^F_{\alpha\beta}(\kappa\kappa',\mathbf{q})-Y^2\phi^C_{\alpha\beta}(\kappa\kappa',\mathbf{q})\ . \tag{A10}$$

$\phi^S_{\alpha\beta}(\kappa\kappa',\mathbf{q})$, $\phi^F_{\alpha\beta}(\kappa\kappa',\mathbf{q})$, and $\phi^C_{\alpha\beta}(\kappa\kappa',\mathbf{q})$ are the shell-shell, core-shell, and Coulomb interactions in the reciprocal space, while K is the core-shell coupling constant of the ion. $M=M_\kappa$ is the mass of the ion κ, $e_\beta(\kappa',\mathbf{q}j)$ is the eigenvector component, and $\omega^0(\mathbf{q}i)$ is the harmonic frequency of the $(\mathbf{q}j)$ mode. In all the cases, $\{l_n\kappa_n\alpha_n\}_{n=1,4}$ refer to unit-cell, atom, and Cartesian indices and $\{\mathbf{q}_n j_n\}_{n=1,4}$ to wave vector and branch index, respectively.

In Eqs. (2.13) and (2.17) we defined, respectively, the following functions:

$$\begin{aligned}\mathcal{P}(\omega,\omega^0(\mathbf{q}j_1),\omega^0(\mathbf{q}j_2))\equiv&\left\{\frac{n(\mathbf{q}j_1)+n(\mathbf{q}j_2)+1}{\omega+\omega^0(\mathbf{q}j_1)+\omega^0(\mathbf{q}j_2)}\right\}_P-\left\{\frac{n(\mathbf{q}j_1)+n(\mathbf{q}j_2)+1}{\omega-\omega^0(\mathbf{q}j_1)-\omega^0(\mathbf{q}j_2)}\right\}_P\\&+\left\{\frac{n(\mathbf{q}j_1)-n(\mathbf{q}j_2)}{\omega-\omega^0(\mathbf{q}j_1)+\omega^0(\mathbf{q}j_2)}\right\}_P-\left\{\frac{n(\mathbf{q}j_1)-n(\mathbf{q}j_2)}{\omega+\omega^0(\mathbf{q}j_1)-\omega^0(\mathbf{q}j_2)}\right\}_P\end{aligned} \tag{A11}$$

and

$$\begin{aligned}\mathcal{D}(\omega,\omega^0(\mathbf{q}j_1),\omega^0(\mathbf{q}j_2))\equiv&[n(\mathbf{q}j_1)+n(\mathbf{q}j_2)+1]\{\delta(\omega-\omega^0(\mathbf{q}j_1)-\omega^0(\mathbf{q}j_2))-\delta(\omega+\omega^0(\mathbf{q}j_1)+\omega^0(\mathbf{q}j_2))\}\\&+[n(\mathbf{q}j_1)-n(\mathbf{q}j_2)]\{\delta(\omega+\omega^0(\mathbf{q}j_1)-\omega^0(\mathbf{q}j_2))-\delta(\omega-\omega^0(\mathbf{q}j_1)+\omega^0(\mathbf{q}j_2))\}\ .\end{aligned} \tag{A12}$$

In Eq. (A11) the subscript P denotes principal part.

[1]B. G. Dick and A. W. Overhauser, Phys. Rev. **112**, 90 (1958).

[2]W. Cochran, Crit. Rev. Solid State Sci. **2**, 1 (1971).

[3]H. Bilz and W. Kress, *Phonon Dispersion Relations in Insulators,* edited by M. Cardona, P. Fulde, and H.-J. Queisser, Springer Series in Solid State Science Vol. 10 (Springer-Verlag, Heidelberg, 1979).

[4]A. Dobry, A. Greco, and O. Zandron, Phys. Rev. B **43**, 1084 (1991).

[5]A. Greco, S. Koval, and R. Migoni, J. Phys.: Condens. Matter **4**, 5291 (1992).

[6]R. A. Cowley, J. Phys. (Paris) **26**, 659 (1965).

[7]G. Dolling, *Slow Neutron Scattering from Solids and Liquids* (IAEA, Trieste/Vienna, 1963), Vol. II.

[8]G. Dolling and R. A. Cowley, Proc. Phys. Soc. (London) **88**, 463 (1966).

[9]A. A. Maradudin and A. E. Fein, Phys. Rev. **128**, 2589 (1962).

[10]E. Haro, M. Balkanski, R. F. Wallis, and K. H. Wanser, Phys. Rev. B **34**, 5358 (1986).
[11]S. Narasimhan and D. Vanderbilt, Phys. Rev. B **43**, 4541 (1991).
[12]C. Z. Wang, C. T. Chan, and K. M. Ho, Phys. Rev. B **40**, 3390 (1989).
[13]H. Tang and I. P. Herman, Phys. Rev. B **43**, 2299 (1991).
[14]W. Weber, Phys. Rev. B **15**, 4789 (1977).
[15]R. A. Cowley, Rep. Prog. Phys. **31**, 123 (1968).
[16]A. A. Maradudin, Phys. Status Solidi **2**, 1493 (1962).
[17]*Intrinsic Properties of Group IV Elements and III-V, II-VI, and I-VII Compounds,* edited by D. Madelung, Landolt-Börnstein, New Series, Group III, Vol. 22a (Springer-Verlag, Berlin, 1987); *Physics of Group IV Elements and III-V Compounds,* edited by O. Madelung, Landolt-Börnstein, New Series, Group III, Vol. 17a (Springer-Verlag, Berlin, 1982).
[18]H. J. McSkimm and P. Andreatch, Jr., J. Appl. Phys. **35**, 2162 (1964).
[19]*Thermophysical Properties of Matter,* edited by Y. S. Touloukian and R. K. Kirby (Plenum, New York, 1975), Vol. 12, p. 116; *ibid.*, Vol. 13, p. 155 (1977).
[20]M. Balkanski, R. F. Wallis, and E. Haro, Phys. Rev. B **28**, 1928 (1983).
[21]A. P. Mayer and R. K. Wehner, Phys. Status Solidi B **126**, 91 (1984).